EARTH SURFACE PROCESSES AND LANDFORMS
Earth Surf. Process. Landforms **41**, 446–459 (2016)

Published online 19 October 2015 in Wiley Online Library
(wileyonlinelibrary.com) DOI: 10.1002/esp.3832

Exploring large wood retention and deposition in contrasting river morphologies linking numerical modelling and field observations

Virginia Ruiz-Villanueva,[1]* Bartłomiej Wyżga,[2,3] Hanna Hajdukiewicz[2] and Markus Stoffel[1,4,5]
[1] Dendrolab.ch, Institute of Geological Sciences, University of Bern, Bern, Switzerland
[2] Institute of Nature Conservation, Polish Academy of Sciences, Kraków, Poland
[3] Faculty of Earth Sciences, University of Silesia, Sosnowiec, Poland
[4] Climatic Change and Climate Impacts, Institute for Environmental Sciences, University of Geneva, Carouge-Geneva, Switzerland
[5] Department of Earth and Environmental Sciences, University of Geneva, Geneva, Switzerland

Received 26 February 2015; Revised 27 July 2015; Accepted 18 August 2015

*Correspondence to: Virginia Ruiz-Villanueva, Dendrolab.ch, Institute of Geological Sciences, University of Bern, Baltzerstrasse 1, CH-3012, Bern, Switzerland.
E-mail: virginia.ruiz@dendrolab.ch

ESPL
Earth Surface Processes and Landforms

ABSTRACT: Large wood tends to be deposited in specific geomorphic units within rivers. Nevertheless, predicting the spatial distribution of wood deposits once wood enters a river is still difficult because of the inherent complexity of its dynamics. In addition, the lack of long-term observations or monitored sites has usually resulted in a rather incomplete understanding of the main factors controlling wood deposition under natural conditions. In this study, the deposition of large wood was investigated in the Czarny Dunajec River, Polish Carpathians, by linking numerical modelling and field observations so as to identify the main factors influencing wood retention in rivers. Results show that wood retention capacity is higher in unmanaged multi-thread channels than in channelized, single-thread reaches. We also identify preferential sites for wood deposition based on the probability of deposition under different flood scenarios, and observe different deposition patterns depending on the geomorphic configuration of the study reach. In addition, results indicate that wood is not always deposited in the geomorphic units with the highest roughness, except for low-magnitude floods. We conclude that wood deposition is controlled by flood magnitude and the elevation of flooded surfaces in relation to the low-flow water surface. In that sense, the elevation at which wood is deposited in rivers will differ between floods of different magnitude. Therefore, together with the morphology, flood magnitude represents the most significant control on wood deposition in mountain rivers wider than the height of riparian trees. Copyright © 2015 John Wiley & Sons, Ltd.

KEYWORDS: wood dynamics; wood transport; in-stream wood; mountain river; Czarny Dunajec

Introduction

Since the early stages of wood research, a plethora of studies has analysed the spatial distribution of large wood (LW), describing the variability of its deposition along river systems and in a wide range of environments (Abbe and Montgomery, 2003; Montgomery *et al*., 2003; Swanson, 2003). These analyses of LW deposition in mountain rivers have shown that complex river morphology and flow patterns play a crucial role in determining potential sites of LW retention (Gurnell *et al*., 2000a, 2000b; Abbe and Montgomery, 2003; Gurnell, 2013). In steep streams with channel gradients between 0.06 and 0.20, most LW deposits comprise pieces anchored on irregularities of channel boundaries (i.e. bedrock outcrops, boulders) or on trees growing along channel margins (Abbe and Montgomery, 2003). In multi-thread rivers, by contrast, LW is preferentially retained on the top of gravel bars, often forming 'bar apex jams' as defined by Abbe and Montgomery (2003). However, island-braided areas may store considerably more LW than bar-braided areas due to greater contact between the active channel and forested islands (Gurnell *et al*., 2002). In large alluvial rivers, by contrast, LW is likely stored along the outer margins of channels, such as concave banks, point bars in meandering rivers, the edges of vegetated islands or the margins of secondary channels (Gurnell *et al*., 2002; Abbe and Montgomery, 2003; Gurnell, 2013). Therefore, geomorphology exerts a major control on the distribution of LW in rivers (Lassettre *et al*., 2008; Morris *et al*., 2009; Wohl and Cadol, 2011) together with other factors such as recruitment processes, forest stand and age (Beckman and Wohl, 2014) or forest and river management (May and Gresswell, 2003; Benda *et al*., 2005; Comiti *et al*., 2006). Stream gradient, channel width and sinuosity are found as the main geomorphic factors controlling the distribution and abundance of LW in rivers (Diez *et al*., 2001; Lassettre *et al*., 2008; Wohl and Jaeger, 2009). In addition, valley side slope, lateral confinement of streams, and longitudinal connectivity within the channel are other important variables in the recruitment and therefore spatial distribution of LW (Wohl *et al*., 2010; Rigon *et al*., 2012). Finally, the hydrologic regime, including flood frequency and magnitude, influences the distribution of LW in rivers as well (Moulin *et al.*, 2011).

With the exception of the uppermost stream reaches where flood discharges are too small to redistribute wood pieces (Gurnell *et al.*, 2002), LW is likely to be non-randomly distributed (Kraft and Warren, 2003; Wohl and Jaeger, 2009). However, predicting the spatial distribution of LW in a river after it enters the system still remains difficult because of the complex interactions among LW recruitment, channel form, and channel hydraulics (Wohl and Cadol, 2011). Improving the understanding of LW retention and distribution is therefore important given the geomorphic and ecological importance of LW in rivers (Gurnell, 2007). Where retained, LW creates and induces formation of a variety of geomorphic features, thus enhancing the complexity of the physical habitat of fluvial systems (Gurnell, 2013).

A variety of techniques have been employed to measure LW retention; these include the detailed mapping of wood pieces (Elosegi *et al.*, 1999; Curran, 2010), remote sensing (Lassettre *et al.*, 2008; Bertoldi *et al.*, 2013), LW tagging and tracking (MacVicar *et al.*, 2009), and physical experiments (Welber *et al.*, 2013; Bertoldi *et al.*, 2014). This paper aims at demonstrating a new approach to predict and analyse LW retention and distribution by combining numerical modelling and field measurements. Recent research illustrates that a wide range of quantitative information about LW transport and deposition can be obtained from the use of numerical modelling together with the proper assessment of boundary conditions and validation based on field data (Ruiz-Villanueva *et al.*, 2014b, 2015). Here we combine two-dimensional hydrodynamic numerical modelling of LW transport and deposition together with field observations and tracking of LW in the river to analyse LW retention along the Czarny Dunajec River in Poland. Two-dimensional numerical modelling was performed here in a multi-run mode, based on multiple scenarios, so that results can be analysed in a probabilistic/statistical manner. The main objectives of this work are thus (i) to determine dominant depositional locations for LW at different discharges in reaches with different geomorphic characteristics, and (ii) to investigate the main factors controlling LW deposition, linking LW retention to river morphology and hydrodynamic conditions.

Study Site

The Czarny Dunajec (Figure 1; Kundzewicz *et al.*, 2014) is a fifth-order river in southern Poland. It drains the Inner Western Carpathians, originating at about 1500 m above sea level (a.s.l.) in the high-mountain Tatra massif, with the highest peak in the catchment at 2176 m a.s.l. The hydrological regime of the river is determined by the high-mountain part of the catchment and is typified by low winter flows and floods occurring between May and August as a result of prolonged frontal rains,

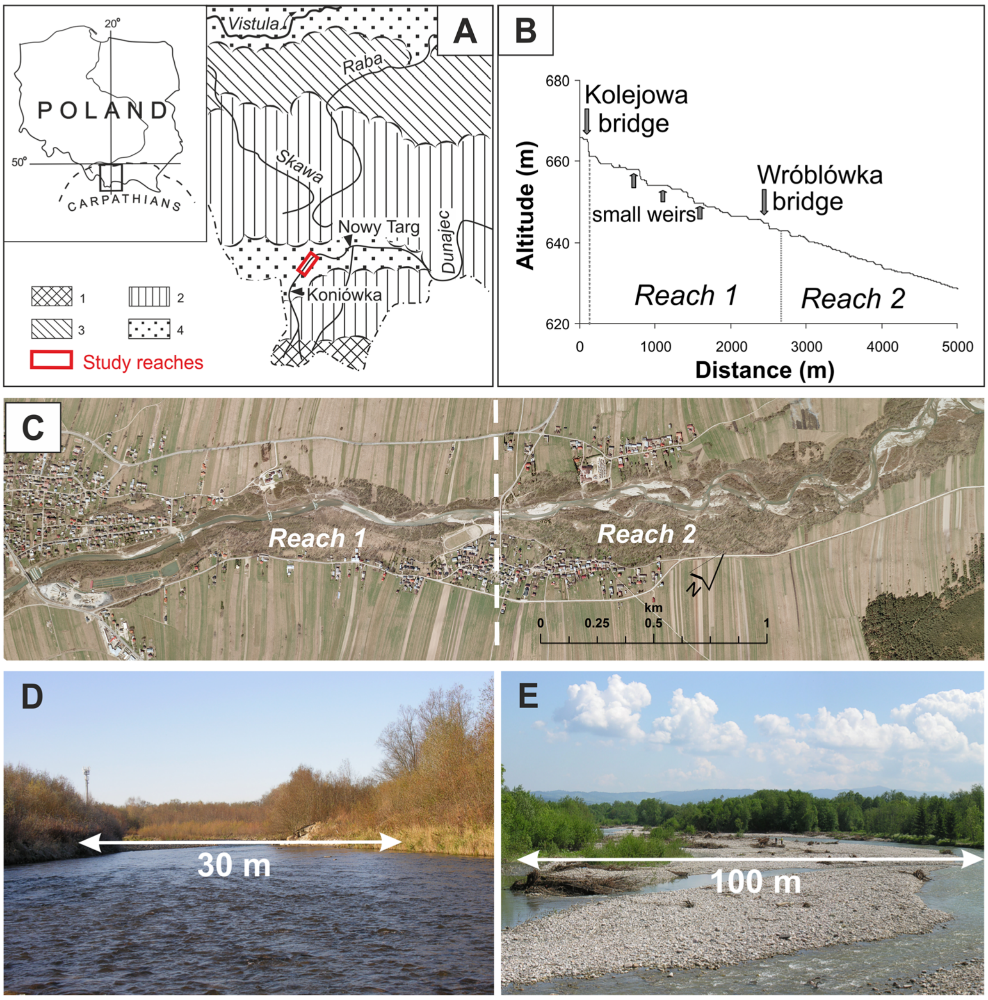

Figure 1. (A) Location of the Czarny Dunajec River and the study reaches in relation to physiogeographic regions of southern Poland. 1 – high mountains; 2 – mountains of intermediate and low height; 3 – foothills; 4 – intramontane and submontane depressions; (B) longitudinal profile of the studied reaches of the Czarny Dunajec; (C) orthophoto from 2009 showing study reaches 1 (D) and 2 (E). Channel widths are indicated in the photographs, but in other parts of Reach 2 the river may be much wider (for details see text). This figure is available in colour online at wileyonlinelibrary.com/journal/espl

sometimes superimposed on snow-melt runoff. Mean annual discharge of the river amounts to 4.4 $m^3 s^{-1}$ at Koniówka, in the middle course of the river (catchment area of 134 km^2), where the model was calibrated; and to 8.8 $m^3 s^{-1}$ at Nowy Targ (432 km^2), close to the confluence of the Czarny Dunajec with the Biały Dunajec River.

In its middle course within the intramontane Orawa-Nowy Targ basin, the river was subjected to spatially variable human impacts over the past decades (Zawiejska and Wyżga, 2010). As a result, it varies highly in width and morphology which in turn allows distinction of two reaches for the modelling of LW transport, namely a single-thread, partially channelized Reach 1 and an unmanaged, multi-thread Reach 2 (Figure 1; Table I). In both reaches, bankfull discharge exceeds a 1.5-year flood (35 $m^3 s^{-1}$). The total length of the reaches is 5.5 km (Figure 1C). In Reach 1, the river has a relatively small, uniform width (Figure 1D) and a few drop structures to reduce slope locally. Channel banks are locally reinforced with gabions or rip rap. In Reach 2, the width of the active river zone amounts to 116 m on average, but varies considerably between 60 m at the upstream end of the reach, where islands are small and scarce (Figure 1E), and about 180 m near its downstream end where islands become more important to represent about half of the total area of emerged surfaces within the active river zone (Mikuś *et al.*, 2013).

The river banks in both reaches as well as the forested islands in Reach 2 are overgrown with forest stands composed of alder and willow species, with predominating young, shrubby forms of *Alnus incana*, *Salix eleagnos*, *S. purpurea* and *S. fragilis*, less frequent stands of older *A. incana* trees and occasional *S. alba* trees (Mikuś *et al.*, 2013). With riparian tree height reaching up to 18 m, the study reaches represent large channels with respect to in-stream wood (Gurnell *et al.*, 2002; Wohl, 2013; Wyżga *et al.*, 2015). The substantial differences in river width between the reaches are reflected in markedly different unit stream power of flood flows and in higher average flow depth in the narrower Reach 1. Moreover, the differences in channel management and river morphology underlie differences in the intensity of LW recruitment and the availability of LW retention sites between the reaches (Wyżga and Zawiejska, 2005, 2010). Field observations carried out after a seven-year flood in 2001 (with a peak discharge of 94 $m^3 s^{-1}$) indicate that the wide, multi-thread sections – where unit stream power was relatively low at flood peak – stored large quantities of LW (up to 33 $t\,ha^{-1}$), whereas the narrow, single-thread sections of the regulated or bedrock channel, typified by high unit stream power, retained markedly lower wood quantities (0.1–1.3 $t\,ha^{-1}$; Wyżga and Zawiejska, 2005, 2010). Data from the wood inventory in 2001 together with field observations performed after subsequent floods, in 2010 and 2014, formed the basis of the current study and were used in the model set-up and verification of results.

Table I. Morphometric and hydraulic parameters of the study reaches

Reach	Geomorphological style	Channel/ active zone width (m)	Longitudinal slope($m\,m^{-1}$)	Length (m)
1	Narrow to moderately wide, single-thread, partially regulated	42	0.007	2300
2	Wide, multi-thread channel, island-braided	116	0.005	3200

Methodology

Coupling hydrodynamics and LW transport: model description

The numerical model presented by Ruiz-Villanueva *et al.* (2014a) was applied to solve the hydrodynamics and to simulate LW transport. This model fully couples a two-dimensional hydrodynamic model based on the finite volume method with a second-order Roe Scheme with a Lagrangian model for wood dynamics. The Lagrangian framework considers logs or wood pieces as specific objects which are tracked through time. The incipient motion of each log is determined by the balance of forces acting on the mass centre of the piece, assuming logs as cylinders. These forces are: (i) the driving forces, including the gravitational force acting on the log, equal to the effective weight of the log in a downstream direction, and the drag force, also acting in the flow direction, which is the downstream drag exerted on the log by the water in motion; (ii) and the resisting forces, including the friction force acting in the direction opposite to flow, which is equal to the normal force acting on the log times the coefficient of friction between the wood and the bed. According to the balance of forces, once the log is put in motion, two possible transport mechanisms are implemented: sliding on the river bed or floating. In all cases, translation and rotation are considered depending on the flow velocity field at the two ends of the log. When the piece of wood is sliding, its velocity will be very different from the flow velocity, with friction being the main control factor of movement. If the log is floating, its velocity will be the same as the flow velocity, unless turbulence is considered. Turbulent fluctuations of velocity affect wood, introducing a random component into the motion of logs. Logs will be transported until resisting forces are higher than driving forces, due to e.g., a reduction of the submerged area (decrease in water depth), or a decrease in flow velocity. In addition, log transport (i.e. velocity and movement) can also be modified when interactions with the river boundary or between logs themselves occur. If one moving piece of wood collides with another piece (both pieces floating or resting), the two continue moving at a different velocity, or they may be deposited. If a piece of wood reaches the bank or a dry area (e.g. floodplain, bars, islands, etc.), the driving forces decrease and the piece can be entrapped. Under these conditions, initial motion is re-calculated. The presence of wood pieces influences hydrodynamics, thereby reducing the available storage volume at every finite volume, and adds a new shear stress (produced by the drag force of the logs). Therefore, the coupling of wood transport and hydrodynamics is solved by adding this additional shear stress term in the Saint Venant equations. For more details about the governing physical equations as well as about the implementation and validation of the model see Ruiz-Villanueva *et al.* (2014a, 2014b, 2014c, 2015).

The numerical model needs initial and boundary conditions for wood. The initial position of each log (x, y coordinates of the mass centre and angle with respect to the flow), its length, diameter and wood density for the initial time step should be provided. Moreover, several inlet boundary conditions (i.e. logs entering the simulation) can also be assigned to the simulation domain boundaries, specifying a number of wood pieces per minute and its characteristics. Based on a detailed knowledge of the fluvial corridor, riparian vegetation, and wood availability, ranges of the main characteristics of logs need to be established: maximum and minimum lengths, diameters and density of wood. Stochastic variations of these parameters together with position and angle are used to characterize the wood entering the domain.

Inlet and boundary conditions: model scenarios

We obtained a detailed (1-m pixel size) geometry of the study reaches by using digital elevation models (DEMs) available from the State Geodetic Survey, and a topographical survey. The topographical survey was performed with a global positioning system (GPS) receiver and a total station with the aim to improve the DEM in those sections where its accuracy was insufficient (i.e. in critical sections such as bridges, dikes or bends). Use of Topcon GRS-1 GNSS controller with PG-A1 antenna together with corrections from reference stations enabled the 0.03 m vertical accuracy of the measurements.

Hydrological data from the closest (i.e. 6.2 km upstream of the studied reaches) stream gauge station (Koniówka) were used to characterize inlet peak discharge of a given return period and to model floods of various magnitudes (Table II). The discharge, assumed as steady-state, was modelled until the model is stabilized; at that time step, LW is entering in the simulation. The rating curve for the station was used for roughness (i.e. Manning *n* coefficient) calibration.

Geomorphic features along the fluvial corridor, homogeneous in terms of their roughness (roughness homogeneous units, RHU), were identified in the field and digitized on the orthophotos using a geographic information system (GIS) environment. Afterwards we assigned a possible range of roughness values (Table III) to each RHU. To do this, we used *in situ* measurements of bed material grain size in selected channel transects surveyed in previous studies (Wyżga *et al.*, 2012; Zawiejska *et al.*, 2015) and we applied different empirical equations relating roughness to grain size (Strickler, 1923; Meyer-Peter and Müller, 1948; Bray, 1979). The calculated roughness values for all RHU (rather than for each RHU separately) were fitted running different discharge ranges (high and low flows) and comparing model results with the rating curve for the Koniówka gauging station. This calibration procedure resulted in an error in water level ranging from 2 to 22.5% for high and low flows, respectively (for more details about calibration results see Ruiz-Villanueva *et al.*, 2015).

Table II. Flood scenarios used to characterize different flood magnitudes in the study reaches

Type of flood	Peak discharge ($m^3 s^{-1}$)	Return period (year)
Very frequent	28	1.2
Ordinary	105	10
Extraordinary	147	25
Extreme	183	50
Very extreme	210	80

Table III. Description of roughness homogeneous units (RHUs), and Manning's *n* coefficient (in $m^{1/2}$ s^{-1}) values used in the model calibration

RHUs	Description	Minimum	Maximum
Forest (F)	Dense stand of willows and alder	0.1	0.15
Gravel and sand (G)	Gravel and sand	0.03	0.05
Shrubs (S)	Medium to dense shrubby trees	0.04	0.08
Meadows/cultivated (C)	Grassland and crops	0.02	0.04
Mature forest (Mf)	Dense stand of large willows and alder	0.1	0.2
Road (R)	Asphalt	0.01	0.014
Scattered trees (St)	Cleared land with some trees stumps	0.05	0.09
Floodplain (Fl)	Mixed between G, S, C	0.03	0.05
BAR	Gravel bars without vegetation	0.07	0.09
IS	Vegetated islands	0.08	0.1
Imf	Forested islands	0.1	0.15
Ih	Islands with shrubs	0.05	0.07
Lfc	Clean low-flow channel with pebbles and cobbles	0.07	0.09

Assuming that LW recruitment is only occurring upstream of the study reaches, a number of logs per minute was defined to enter the simulation. We are well aware that LW may also be recruited from eroded river banks, particularly in Reach 2, but this possible erosion has not been taken into account in our simulations. This simplification should be considered when model results are analysed. In any case, the exact number of logs entering the river reach is simply an approximation, although we set values that are reasonably consistent with qualitative observations made during field inventories (Wyżga and Zawiejska, 2005, 2010); we treat the results from a relative perspective by using a probabilistic approach.

To characterize each piece of LW entering the simulation, we established ranges of maximum and minimum lengths, diameters, and wood density. Stochastic variations of these parameters together with the position and angle with respect to flow were then used. All ranges among the main types of trees recruited to this river were covered, namely:

(i) Type 1 – large trees:
  (a) Type 1A represents large alders (*Alnus incana*) and mature willows (*Salix eleagnos*) with single trunk, relatively small crowns, 10 to 15 m in height, and 0.15 to 0.3 m in diameter. At the study sites, type 1A trees grow in sub-mature to mature forest on the river banks and older islands, where they constitute about 90% of trees. In the study river, type 1A trees produce logs of simple geometry after their recruitment to the river.
  (b) Type 1B: large willows with a single trunk and a large, three-dimensional crown (*Salix fragilis* and *S. alba*). Such trees will typically be transported over only very short distances. These trees are not subjected to disintegration but may form the nuclei of wood jams. Along Reach 2, type 1B trees constitute about 10% of the vegetation in sub-mature to mature forest on the river banks and on older islands (length 10–18 m; diameter 0.3–0.8 m).

(ii) Type 2: Young willows (especially *Salix purpurea* and *S. eleagnos*) and alder growing on younger islands and in young forests on the river banks. They are typically 3–10 m in height. Their relatively thin stems and branches can be broken easily during transport, thus providing much of the material subsequently aggregated and stored in jams. Sometimes, when they show a more complex geometry, they can be anchored at any obstacle such as wood jams, trees growing on islands or at channel margins (but also at bridge piers). This type was simulated as medium logs (3–10 m in length and 0.1–0.2 m in diameter).

(iii) Type 3 representing branches broken from stems and crowns, mainly from type 1 and 2 trees; they are simulated as logs 1–3 m in length and 0.05–0.1 m in diameter.

Combining all the different log types and the defined flood discharges for Reaches 1 and 2 resulted in the final set of model runs consisting of 72 scenarios. Scenarios were designed to be in agreement with the characteristics of the river.

To analyse the geomorphology as a factor controlling wood retention (Gurnell *et al*., 2000a, 2000b), the two reaches investigated in this study were chosen so as to show contrasting geomorphic configurations.

Data analysis and field observations

We explored the main controls on LW retention and deposition by applying multiple model runs. Results were first analysed in terms of the retention capacity (Rc). Here Rc is defined as the ratio between deposited logs and inlet number of logs (Rc = deposited logs/inlet logs) which is inverse to the wood transport ratio (Tr = pieces transported downstream the study reach/total inlet logs; Tr = 1 − Rc) defined in Ruiz-Villanueva *et al*. (2015). The analysis of the preferential sites for deposition was based on the probability of logs to be deposited on a specific RHU. Results from all the 72 scenarios indicated the proportions of logs deposited at one place, and we used this to compute depositional probability (probability of deposition occurrence). Calculating LW deposition as the probability of occurrence is very advantageous because it allows for easy comparison between the two study reaches or different scenarios for the same reach.

We then analysed the relative elevation of simulated wood deposits above low-flow water surface and above the lower channel bank. For each model run, sites with LW deposition were projected on channel centreline, the boundary of low-flow channel and channel banks. The intersection of the projection line with the channel centreline indicated the position of each depositional site along the investigated reaches. The altitude of deposition sites was read from the DEM and compared with that of the intersection points of the projection lines with a low-flow channel boundary, hence providing information about the relative elevation of each LW deposit above the low-flow water surface in the reaches. The height of both channel banks in the channel cross-sections with LW deposits was determined and the lower of the two channel banks was considered in further analysis. Finally, the elevation of each depositional site in relation to the lower channel bank was established by comparing their altitudes derived from the DEM.

Next, relations between LW depositional probability and potential controlling variables were investigated. Because the application of the Shapiro–Wilk test indicated non-normal distribution of residuals from simple linear regressions, this type of analysis was invalid and a non-parametric approach had to be employed. The Spearman rank correlation test was thus applied to test correlation between LW depositional probability and individual controlling variables, whereas the dependence of depositional probability on multiple controlling variables was verified by means of generalized multiple regression analysis (linear regression models that allow for variables with non-normal distribution of residuals). The generalized multiple regression analyses were accomplished by means of the backward stepwise procedure, which generates regression models in which the choice of predictive variables is carried out by the p-value < 0.05. The considered controlling variables comprised Manning n roughness coefficient of depositional sites, flow velocity and log characteristics (i.e. diameter, length, and wood density). Because the model runs were performed independently for each reach and at least some statistical samples had non-normal distribution, we used the non-parametric Mann–Whitney test to verify whether the two study reaches differ in a given parameter. To test differences in a given parameter among different flood scenarios, the Kruskal–Wallis test was used. In addition to testing differences in the median, we tested differences in the cumulative distribution with a bootstrap version of the univariate two-sided Kolmogorov–Smirnov test. Correlations and differences were considered statistically significant if p-value < 0.05. The R-Statistical (version 3.1.2; www.r-project.com) program and the Statistica software were used for the statistical analyses.

All results regarding LW dynamics were, whenever possible, validated and compared to direct observations. Field observations regarding LW deposition were performed after significant floods that had occurred recently in the river in 2001, 2010, and 2014.

During the last flood on record in May 2014, 30 logs tagged with radio transmitters were placed into the river just before the flood peak. The tagged logs were similar to those defined as type 1A, but shorter for logistical reasons, with log length of 3 m and diameter of about 20 cm. The flood had a peak discharge of 130 $m^3 s^{-1}$, which corresponds to a 20-year recurrence interval at Koniówka gauging station, so it falls between the ordinary and extraordinary flood categories distinguished in Table II. At this magnitude, flow is high enough to overtop Reach 1 and to activate all low-flow channels and inundate gravel bars and islands in Reach 2.

The signal of the radio transmitters could be traced at a distance of 2 km, and we recovered 80% of the logs. Logs that were not recovered were excluded from further considerations. Tracking deposited logs allowed further verification of our model results. The number of logs considered to enter a given reach was thus determined by the total number of logs placed in the river upstream of this reach minus those not recovered and those deposited upstream of the reach. We thus could calculate the deposition ratio in a given reach for the tagged logs.

Results

Preferential sites of LW deposits and wood retention capacity

Depositional probability strongly depends on flood magnitude and the geomorphic configuration of the river. Figures 2 and 3 demonstrate that for each flood scenario and for each river reach, different values and different spatial distributions were obtained in terms of LW depositional probability.

Figure 2 shows that in the case of single-thread Reach 1 and for low-magnitude, high-frequency floods, the preferential sites for LW deposition are the main channel, bars and the forested areas adjacent to the main channel. During such floods, LW delivered to the reach will not be transported downstream because of insufficient flow energy or excessive log dimensions and will thus be deposited in these geomorphic features.

As flood magnitude increases, the probability for LW to be deposited in the main channel of Reach 1 decreases, and LW is likely to be transported downstream of this reach or is deposited in the areas located at some distance from the main channel which are typically covered by mature forest. This pattern was observed after the flood of May 2014, during which only a single log out of the 11 tagged logs entering the Reach 1 was in fact also deposited in Reach 1. During very extreme floods, by contrast, water will inundate the floodplain and a proportion of wood pieces will be directed onto the channel banks where the flow is shallow and slow.

In the case of the multi-thread channel (Reach 2), the depositional probability depends on flood magnitude as well, but we also observe higher variability (Figure 3). This reach is typified by greater complexity of flow pattern and a proportion of the active river zone is covered by island surfaces at the expense of open gravel areas. During frequent floods, bars,

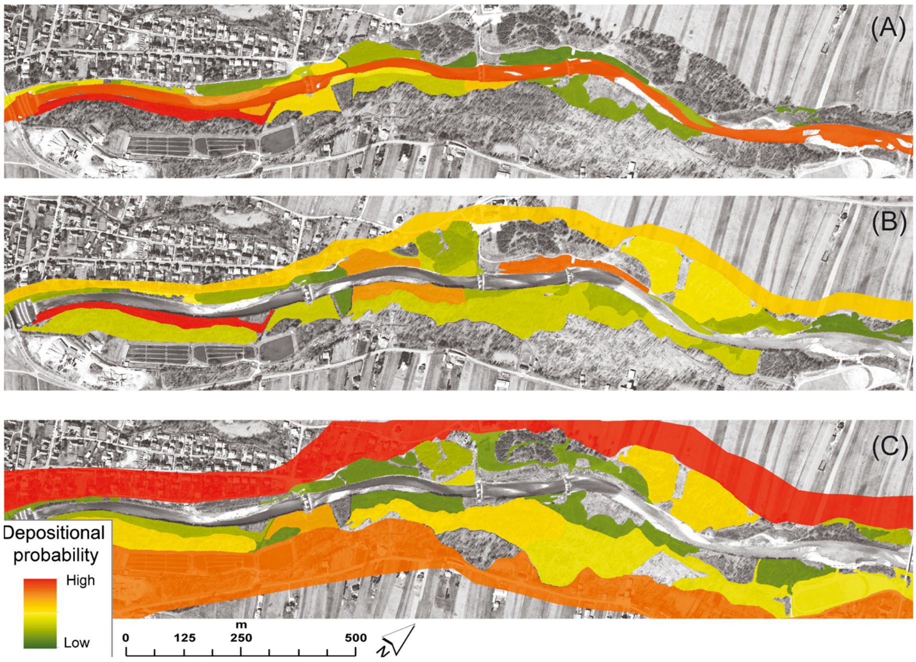

Figure 2. Map of the probability of large wood (LW) deposition in the single-thread Reach 1 for different flood scenarios: (A) frequent flood (1.2-year flood with a peak discharge of 28 $m^3 s^{-1}$); (B) ordinary flood (10-year flood; 105 $m^3 s^{-1}$); (C) very extreme flood (80-year flood; 210 $m^3 s^{-1}$). Flow direction is from left to right. This figure is available in colour online at wileyonlinelibrary.com/journal/espl

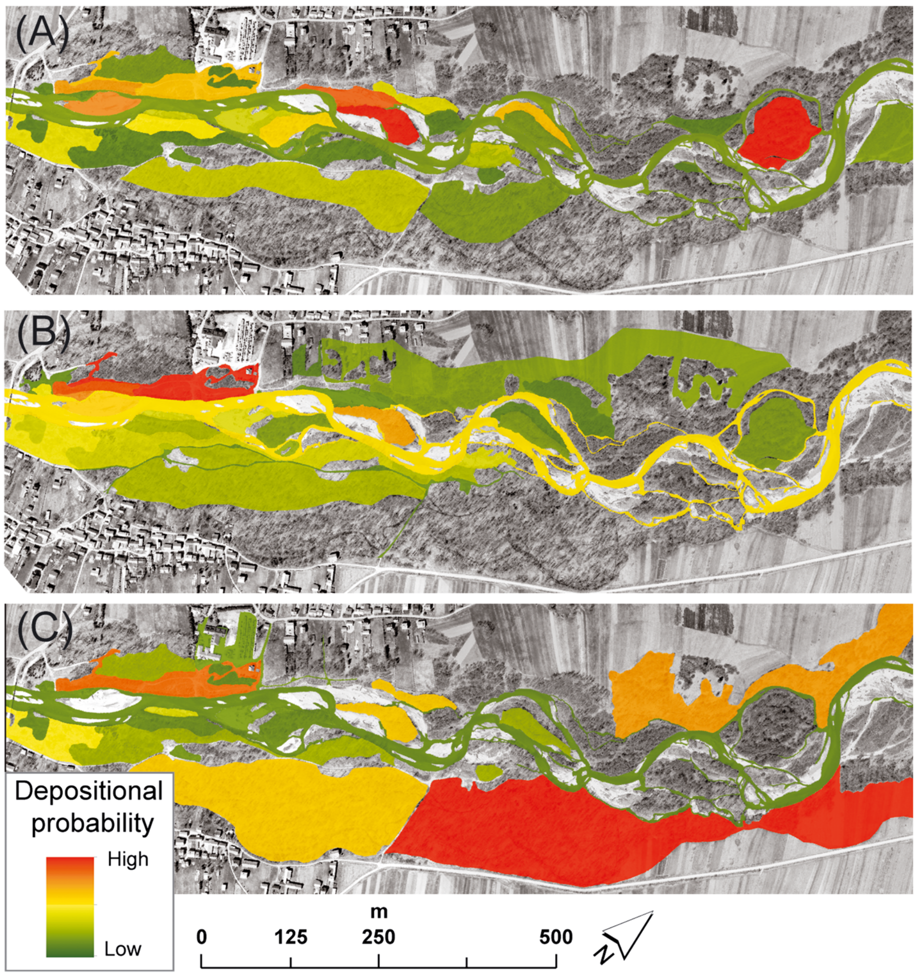

Figure 3. Map of the probability of large wood (LW) deposition in the multi-thread Reach 2 for different flood scenarios: (A) frequent flood (1.2-year flood with a discharge of 28 $m^3 s^{-1}$); (B) ordinary flood (10-year flood; 105 $m^3 s^{-1}$); (C) very extreme flood (80-year flood; 210 $m^3 s^{-1}$). Flow direction is from left to right. This figure is available in colour online at wileyonlinelibrary.com/journal/espl

vegetated islands, and forested islands are the preferential sites for LW deposition, whereas LW is not deposited on the floodplain. This depositional pattern was observed after the 2001 flood with a discharge of 94 $m^3 s^{-1}$ and a seven-year recurrence interval; when no LW was retained within the floodplain as the flood flow was conveyed within the limits of the active zone. LW was instead mainly found to be deposited at the head of vegetated islands, along the margins of forested islands – which trapped LW as lateral ribbons parallel to the low-flow channel – and at bar crests, where flood flow was too shallow to enable flotation (Wyżga and Zawiejska, 2005). Modelling results indicate that in the case of ordinary floods (>10-year recurrence interval), LW will be preferentially deposited on forested islands, in mature forests and crops on the floodplain, and along the margins of braids (including the main channel), whereas during very extreme floods it will be retained far away from the main channel and the active river zone, more precisely in areas covered by meadows and crops as well as in mature forests. Due to the relatively flat cross-sections of this reach, small changes in flood discharge and water level result in large variations of flooded area, thus determining a wider lateral dispersion of LW pieces as observed in Figure 3.

In Reach 1, LW depositional probability during frequent and ordinary floods is higher along the right bank, whereas during very extreme floods LW retention will be higher on the left side of the river. In turn, the left side of the river is more prone to retain LW during frequent and ordinary floods in Reach 2, whereas during very extreme floods the right side exhibits greater potential for LW retention. In general terms, the roughness coefficient of these areas does not change with changes in flood magnitude, at least in the simulation runs. In reality, however, roughness may change if, for instance, vegetation is bent to the ground during a flood, but this hypothetical situation has not been taken into account in the simulations. Instead, we argue that the reason for the high probability of LW deposition in these different areas is related to the depth of floodplain inundation, which is different on the left than on the right river side in both reaches.

We also observe that LW retention capacity differs significantly between both reaches (Mann–Whitney test, $p = 0.002$), with higher values being observed in the multi-thread as compared to the single-thread channel. This observation is consistent for all flood scenarios and log types considered in this study (Figure 4). The retention capacity of Reach 1, averaged for all scenarios, is 0.57 [standard deviation (SD) = 0.21]. This means that 57% of the LW pieces entering the river reach are deposited and not transported downstream. In turn, Reach 2 shows an average retention capacity of 0.74 (SD = 0.17), so that 74% of the inlet logs are deposited within this reach.

Preferential sites for wood deposition and depositional probability vary significantly between the reaches and flood scenarios as well (Figure 5). For frequent floods, depositional probability is higher in Reach 1, for ordinary floods it is similar in both reaches, and for very extreme floods it is slightly higher in Reach 2. In all cases, however, smaller quantities of LW will likely be retained in Reach 1 as compared to Reach 2, but preferential sites for LW deposits are also less numerous in Reach 1, such that the relative probability to be deposited is also higher there.

The recent tracking of tagged logs and observations after floods in 2001, 2010, and 2014 allowed comparison of model results with field data and illustration of depositional conditions for both reaches during relatively high-magnitude floods. From all logs placed in the river during the flood of May 2014, only one was deposited in Reach 1, thus confirming the low

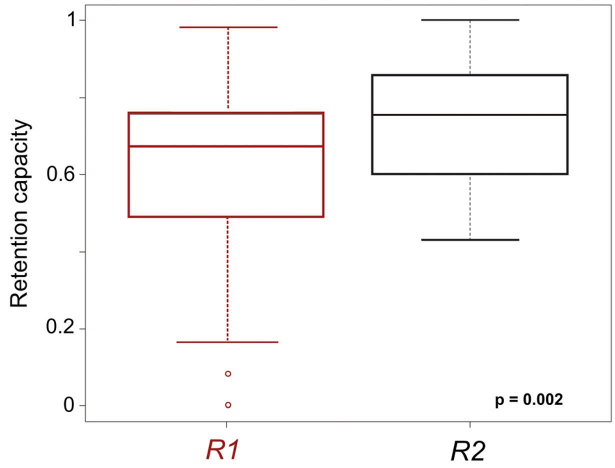

Figure 4. Boxplot of the range of retention capacity values obtained for various discharges for the single-thread Reach 1 (R1) and multi-thread Reach 2 (R2). The bottom and top of the box indicate the first and third quartiles, respectively, the line inside the box is the median and circles are outliers. The Mann–Whitney test for the significance of difference between the means of retention capacity in both reaches is given as well. This figure is available in colour online at wileyonlinelibrary.com/journal/espl

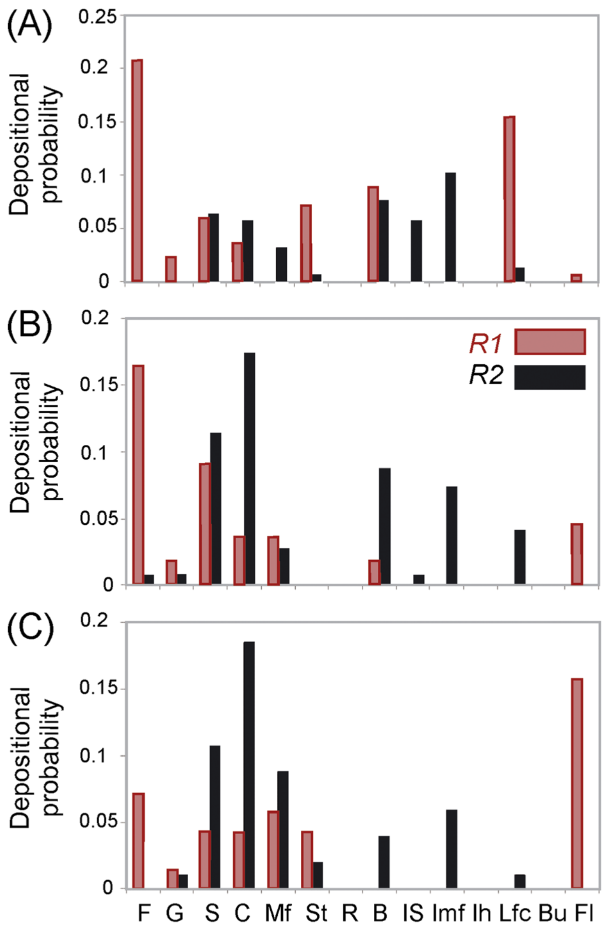

Figure 5. Depositional probability values for different roughness homogeneous units (RHUs): forest (F), gravelly and sandy surfaces within the floodplain (G), shrubs (S), meadows/cultivated land (C), mature forest (Mf), road (R), building (Bu) (buildings are included in the geometry of the model, only small and isolated constructions are, however, represented by high roughness values), scattered trees (St), gravel bars without vegetation (B), vegetated island (Is), Forested island (Imf), Island with shrubs (Ih), Low-flow channel (Lfc), Floodplain (Fl); and for different flood scenarios: (A) frequent floods; (B) ordinary floods; (C) very extreme floods. This figure is available in colour online at wileyonlinelibrary.com/journal/espl

retention capacity of the single-thread river reach. Since this particular log was retained below the water surface, we illustrated depositional conditions in Reach 1 with a log found in another river reach with similar geomorphic configuration (with the latter being deposited downstream of the studied reaches; Figure 6A). The log was deposited on the 2-m-high margin of the narrow, regulated channel, in a side part of a wood jam. By contrast, more than half of the tagged logs were deposited in Reach 2, inside the riparian forest (Figure 6B), on an island margin (Figure 6C) and on an island head (Figure 6D).

Factors controlling LW deposition

The geomorphic units where LW is preferably deposited change with peak discharge and thus depend on flooded area. The geomorphic units were characterized by specific values of the roughness coefficient (RHU). Cumulative frequency distributions further illustrate the roughness values of the RHU where simulated LW is deposited, and those of the flooded geomorphic units (i.e. potential sites for deposition) in a particular river reach and for a given flood scenario. We observed statistically significant differences in LW deposition (according to the Kolmogorov–Smirnov test) between the two distributions for most of the analysed discharges (Figure 7).

The first observation refers to a disparity in roughness coefficient values for the sites with LW deposits and flooded units at both river reaches and for the three flood scenarios. However, this divergence is reduced for very extreme floods ($p > 0.05$). In Reach 1, the area flooded during frequent floods is mainly limited to the main channel and bars. More than 50% of the geomorphic units flooded at the peak discharge of $28\,m^3\,s^{-1}$ have roughness values around $0.09\,m^{1/2}\,s^{-1}$, whereas only a small percentage of geomorphic units have higher (mainly forested banks) or lower (mainly areas covered by shrubs or meadows) roughness values. However, at those sites where LW is deposited, the distribution of roughness values varies because LW is deposited not only along the main channel but also on the bars and along the forested banks. During ordinary floods, the flooded area is extended to the floodplain so that the percentage of flooded units with low roughness values is higher than in the low-magnitude flood scenario. These low-roughness units are mainly areas covered by crops, areas covered by shrubs and the areas consisting of a mixture of these land-use types and/or sandy-gravelly surfaces of unpaved roads. The variability in roughness values of LW deposition sites during frequent and ordinary floods is also higher, although more than 50% of the sites where LW is deposited have roughness values lower than $0.05\,m^{1/2}\,s^{-1}$. However, the percentage of depositional sites with high roughness is also increased (around 30%), as a proportion of the LW pieces are also deposited in the area covered by mature forest. For extreme floods, we observe the highest variability in roughness values; LW is then deposited mainly along the floodplain and in the forested areas far away from the channel, and only a small percentage is deposited on bars.

The frequency distribution for Reach 2 is slightly different than for Reach 1, despite the fact that variability in roughness values in Reach 2 also increases with increasing flood magnitude and the disparity of roughness values for flooded areas and LW deposition sites decreases with the increase in peak discharge. For low-magnitude floods, flooded areas are mainly restricted to the main channel and side braids, bars and some islands, with LW deposition taking place on bars and islands. This is the only case where LW is quite obviously deposited in areas with the highest roughness values within the flooded area. By contrast, during ordinary and extreme floods, LW is deposited in areas covered by crops and shrubs along the floodplain, which have lower roughness than forested islands or bars, thus providing evidence that locations of LW deposition depend on flood magnitude and that deposition does not always occur in those features where roughness is highest (Figure 8).

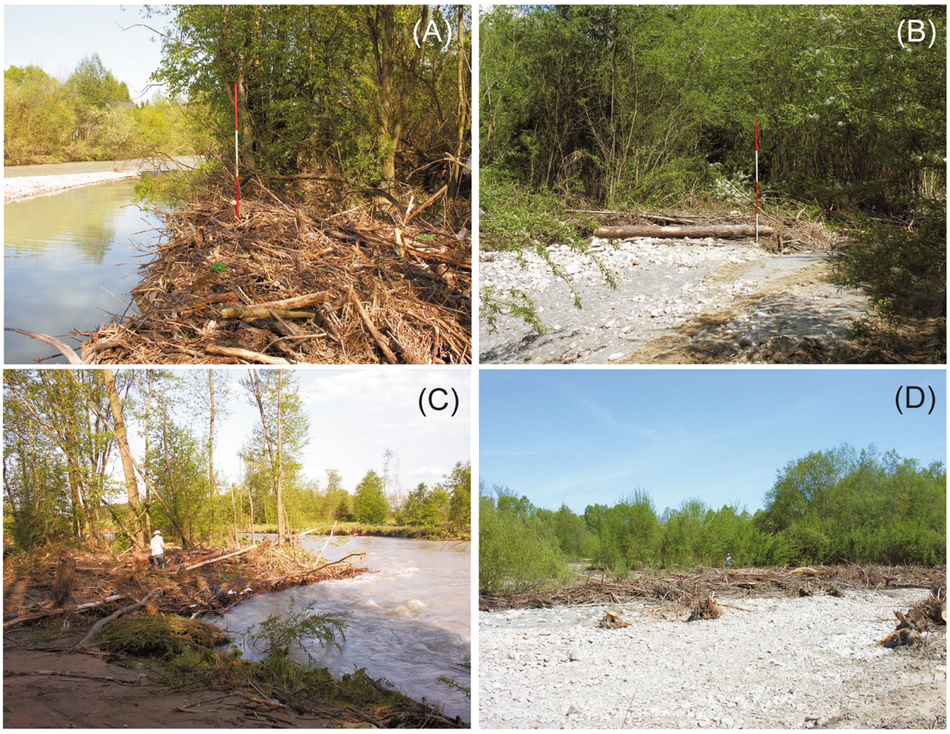

Figure 6. Pictures taken after the flood of May 2014 showing tagged logs deposited during the event. (A) The log found in a narrow, channelized reach illustrates characteristic depositional conditions of Reach 1, as explained in the text. (B–C) Logs deposited in Reach 2: inside the riparian forest (B), on an island margin (C) and in a large jam on an island head (D). This figure is available in colour online at wileyonlinelibrary.com/journal/espl

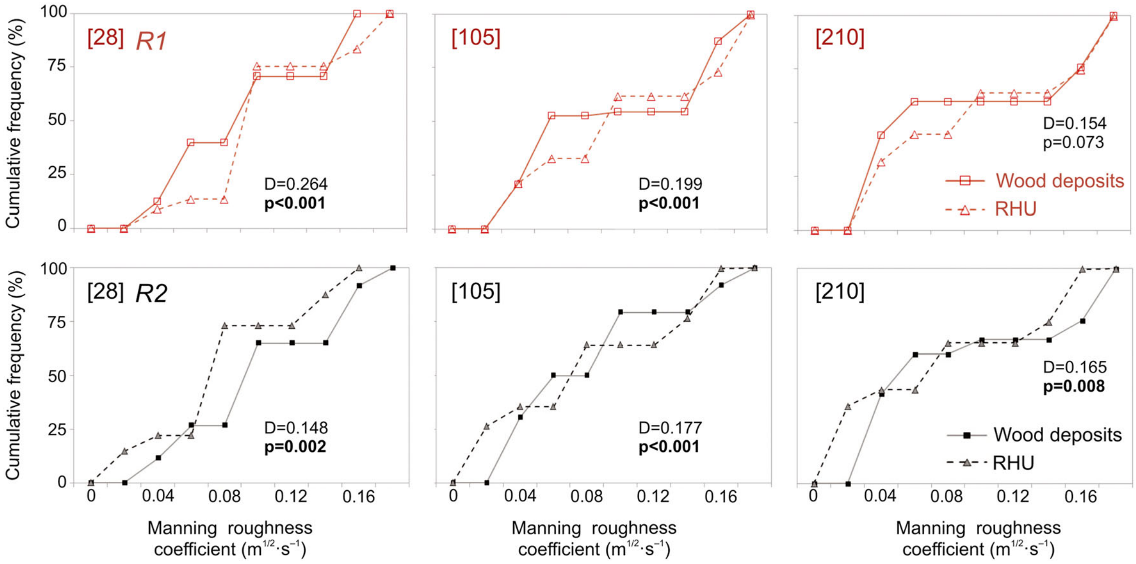

Figure 7. Cumulative frequency distributions for roughness values of the sites with wood deposits (solid lines) and the flooded roughness homogeneous units (RHUs) (dotted lines) in Reach 1 (R1) and Reach 2 (R2) as identified for different flood scenarios: frequent (28 $m^3 s^{-1}$), ordinary (105 $m^3 s^{-1}$), and very extreme (210 $m^3 s^{-1}$) floods. Results of the Kolmogorov–Smirnov test for the significance of differences between the distributions are also indicated. *p*-Values < 0.05 are shown in bold. This figure is available in colour online at wileyonlinelibrary.com/journal/espl

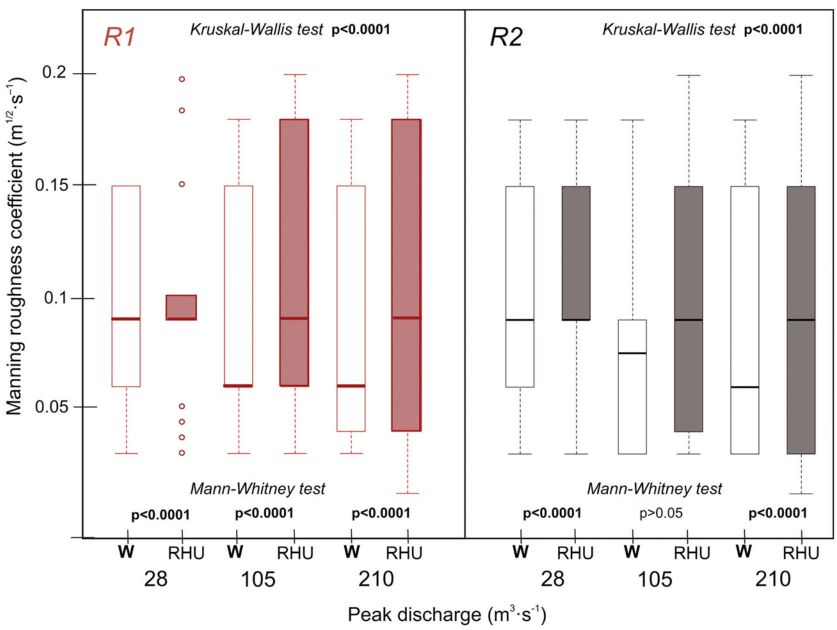

Figure 8. Boxplot graphs of roughness values of sites with large wood (LW) deposits (W) and flooded geomorphic features (RHUs) in Reach 1 (left graphs) and Reach 2 (right graphs) at different peak discharges. For details see Figure 7. Results of the Mann–Whitney test for the difference between sites with LW deposits and flooded units at particular flood discharges and of the Kruskal–Wallis test for the differences among LW depositional sites and flooded units at all analysed flood magnitudes are also indicated. *p*-Values < 0.05 are shown in bold. This figure is available in colour online at wileyonlinelibrary.com/journal/espl

Results from the Spearman correlation analysis indicate that LW depositional probability is related to log dimensions (length and diameter), wood density, Manning's roughness coefficient of depositional sites or RHUs, and flow velocity (Table IV). Water depth has not been included among the independent variables because similar to flow velocity, water depth equalled zero at most deposition locations.

The same variables were then used in the stepwise multiple regression analysis. The obtained models point to the decisive role of either log length or log diameter, and Manning's roughness coefficient of a given surface. At the same time, however, we observe that the direction of the relationship differs between low- and high-magnitude floods. For low flood flows ($Q = 28\ m^3 s^{-1}$) in single-thread Reach 1, variation in depositional probability (DP) was best explained by the following generalized linear relationship with Manning's roughness coefficient:

$$DP = -3.991 + 13.842 \times \text{Manning}$$

The equation indicates that during low flood flows depositional probability is higher in areas with higher roughness within the flooded area. In the case of very extreme floods ($Q = 210\ m^3 s^{-1}$) in reach 1, the following equation was obtained:

$$DP = -2.370 - 1.708 \times \text{Diameter} - 4.859 \times \text{Manning}$$

Table IV. Results of Spearman correlation between wood depositional probability and the parameters characterizing wood pieces and hydrodynamic conditions at the depositional sites in Reach 1 and Reach 2 and during very frequent and very extreme floods

Flood magnitude	Very frequent flood		Very extreme flood	
Independent variable	Spearman correlation	*p*-Value	Spearman correlation	*p*-Value
Reach 1				
Wood density (g cm^{-3})	*0.156*	*0.043*	−0.031	0.797
Piece diameter (m)	*0.283*	*0.007*	*−0.229*	*0.057*
Piece length (m)	0.147	0.057	−0.180	0.137
Manning roughness coefficient (m$^{1/2}$ s^{-1})	*0.638*	*<0.001*	−0.219	0.068
Flow velocity (m s^{-1})	[a]	[a]	0.011	0.927
Reach 2				
Wood density (g cm^{-3})	*−0.160*	*0.044*	*−0.358*	*<0.001*
Piece diameter (m)	*−0.283*	*<0.001*	*−0.458*	*<0.001*
Piece length (m)	*−0.324*	*<0.001*	*−0.488*	*<0.001*
Manning roughnesscoefficient (m$^{1/2}$ s^{-1})	*0.258*	*0.001*	*−0.468*	*<0.001*
Flow velocity (m s^{-1})	*−0.336*	*<0.001*	0.088	0.380

Note: Correlations with p values < 0.05 are indicated in italic typeface.
[a]During very frequent floods in Reach 1, wood is mainly deposited in dry sites where flow velocity equals zero, which renders an estimation of correlation impossible.

indicating that LW depositional probability is negatively related to both Manning's roughness coefficient and log diameter. The depositional probability is thus higher in areas with low surface roughness. The negative relation between depositional probability and log diameter can be explained by the fact that with a mean length of simulated pieces at 12.5 m, even thin logs can interact easily with and be anchored on the margins of the narrow, single-thread channel. By contrast, in the case of shorter pieces, interactions with the channel margins are less likely and the ratio between log diameter and water depth will be high enough to allow their downstream transport, even if the logs have large diameters.

In the case of low flood flows ($Q = 28\,\mathrm{m^3\,s^{-1}}$) in multi-thread Reach 2, the variation of depositional probability was described by the equation:

$$\mathrm{DP} = -3.154 + 3.514 \times \mathrm{Manning} - 0.044 \times \mathrm{Length}$$

Similar to Reach 1, depositional probability was also higher in the areas with higher roughness within the flooded area. The equation also indicates that longer wood pieces are generally less likely to be deposited in this reach, although a more detailed inspection of results for this scenario reveals a more complicated pattern. Shorter pieces (up to 8 m) are more easily deposited than longer pieces (between 8 and 16 m) as the flow readily introduces shorter pieces to shallow channel areas, whereas longer pieces, with greater momentum, tend to be transported along the thalweg. In turn, very long logs (from 16 m up to 22 m) are also easily deposited in Reach 2 as their length facilitates their anchoring on the margins of particular braids.

In the scenario describing a very extreme flood ($Q = 210\,\mathrm{m^3\,s^{-1}}$) in Reach 2, the variation in depositional probability was explained by the following relationship:

$$\mathrm{DP} = -1.700 - 3.589 \times \mathrm{Manning}$$

indicating a negative relation with the surface roughness. This observation again reflects the fact that LW is mostly deposited in areas with lower roughness coefficient values (i.e. on the floodplain) in the case of extreme discharge.

According to these results, depositional probability is related to the roughness of depositional sites in all scenarios and for both reaches; however, they also indicate that the direction of the relationship changes with flood magnitude (Table V). In

Table V. Results of the Spearman rank correlation analysis between wood depositional probability and Manning's roughness coefficient at sites with large wood (LW) deposits in Reach 1 and Reach 2 and for different flood scenarios

	Reach 1		Reach 2	
Flood magnitude	Spearman correlation	*p*-Value	Spearman correlation	*p*-Value
Very frequent (28 m^3 s^{-1})	0.638	<0.001	0.258	0.001
Ordinary (105 m^3 s^{-1})	0.279	0.003	*−0.418*	<0.001
Very extreme (210 m^3 s^{-1})	*−0.219*	0.068	*−0.468*	<0.001

Note: Negative correlations are highlighted in italic typeface.

Reach 1 characterized by a relatively deep channel, the relationship reverses at considerably higher flood flow (Table V).

The location of LW deposition is influenced not only by the roughness of a given area, but also by log shape and peak discharge of a flood. The flood magnitude controls water depth and therefore defines depositional elevations. The roughness coefficient of the floodplain is lower than that of the mature forest on islands, but typically the elevation of the floodplain is also higher than the elevation of island surfaces. Therefore, during larger floods, logs may float into islands, while be deposited after they enter the floodplain area.

Therefore, wood deposition is not only linked to roughness, or to roughness-related flow resistance, but also to the relative position or elevation of depositional sites within the river or floodplain for a given flood scenario. The relative elevation of LW depositional sites was considered with respect to (i) the low-flow water surface (Elev. LFS) and (ii) the lower river bank (Elev. LRB). These relative elevations were analysed for each reach and different peak discharges of flood waves (Figure 9).

For all flood magnitudes, the average elevation of LW deposits above the low-flow water surface is higher in the single-thread Reach 1 with its narrow and deep channel than in the multi-thread Reach 2 with its wide and shallower channel. In both reaches, the relative elevation of LW deposits changes significantly with changing flood magnitude (Figure 9). In a similar way, elevation of LW deposits relative to the lower river bank also depends significantly on flood magnitude.

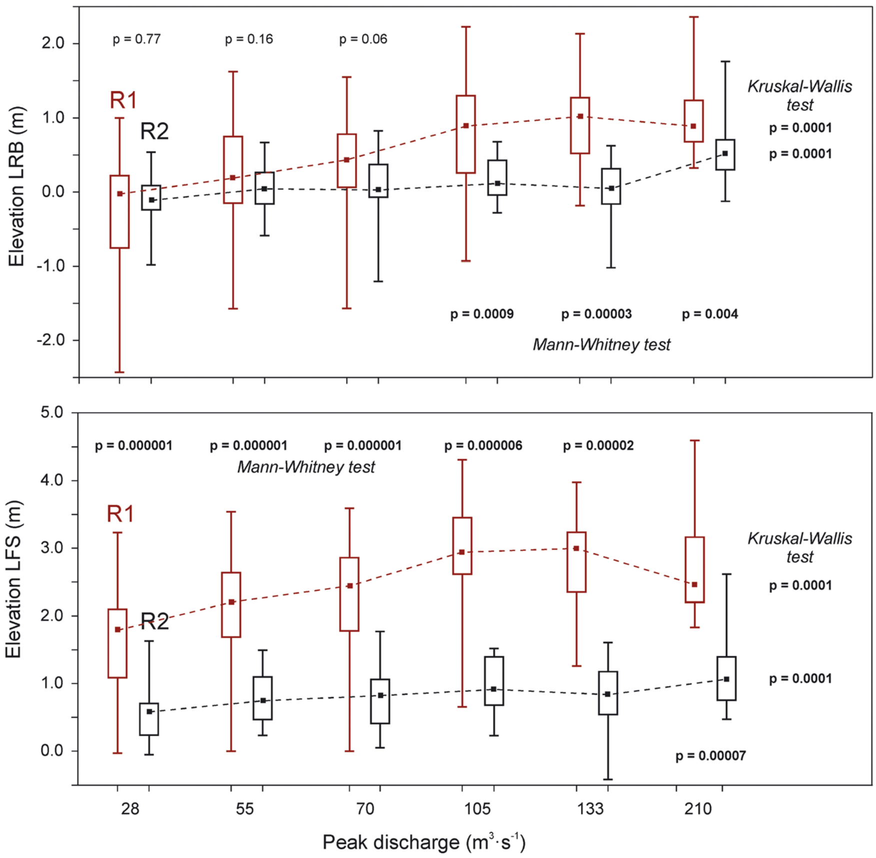

Figure 9. Elevation of large wood (LW) deposition relative to the lower river bank (LRB; upper diagram) and low-flow water surface (LFS; lower diagram) in Reach 1 (R1) and Reach 2 (R2) at different peak discharges. *p*-Values under/below the graphs indicate statistical significance of differences between the reaches determined by a Mann–Whitney test, and those on the right side give differences among different peak discharges in a given reach determined by the Kruskal–Wallis test. *p*-Values < 0.05 are shown in bold. This figure is available in colour online at wileyonlinelibrary.com/journal/espl

However, in case that the relative elevation of LW deposits is considered, differences between the two reaches apparently increase with increasing flood magnitude, but become statistically significant once a certain flood magnitude is attained (Figure 9).

Discussion

In this paper we explored LW retention and deposition in a wide mountain river by linking numerical modelling and field observations. Numerical modelling is a valuable tool to analyse different aspects that govern LW deposition, and allows computation of LW depositional probability. Moreover, numerical modelling predicts the spatial distribution of LW deposits. In the case study presented there, model results are generally similar to field observations and tracking experiments performed in the Czarny Dunajec River after floods. This demonstrates that numerical modelling not only represents a valuable tool to study different mechanisms governing LW deposition, but that it also has the potential to capture processes adequately, despite the fact that some limitations inherent to models persist [see the discussion in Ruiz-Villanueva *et al.* (2014a) for details].

Preferential sites for LW deposition were identified based on the probability of deposition computed by a multi-run model approach, and we observe that depositional probability strongly depends on the geomorphic configuration of the river. We also observe a longitudinal variation in depositional probability within the study reaches. This observation reflects the fact that we only simulate LW recruitment from upstream of the study reaches, so that LW was not always transported along entire reaches, or travelling long distances, but deposited close to its source, except for very extreme floods. In this sense the model represents a simplification of reality, in particular for Reach 2 where LW recruitment from eroded channel and island margins can indeed be very important.

We also observe that the morphological configuration of the river has a clear influence on LW retention capacity that is found to be higher in the multi-thread channel. This different potential of both reaches to retain LW was confirmed during LW inventories performed after the floods in 2001 and 2010, where Wyżga and Zawiejska (2010) showed that LW deposits retained in Reach 2 were more abundant and larger than in Reach 1. Similar observations were also reported by other researchers in similar fluvial environments. By way of example, wood storage was observed to vary significantly between different geomorphic configurations (island-braided and bar-braided reaches) of the Tagliamento River in Italy (van der Nat *et al.*, 2003), whereas in the Piave River (Italy), Pecorari (2008) reported higher storage in braided as compared to wandering reaches. In general, braided rivers are characterized by specific width/stage relationships where relatively small increases of water depth are associated with major widening of wet area (van der Nat *et al.*, 2002; Welber *et al.*, 2013). As a consequence, wood is easily dispersed (Bertoldi *et al.*, 2013).

Other authors have previously reported geomorphic units which are more likely to retain LW within rivers (Piégay *et al.*, 1999; Gurnell *et al.*, 2000a, 2000b; Montgomery *et al.*, 2003). According to our findings, LW is more likely to be deposited along the main channel, on point bars and in the forested areas adjacent to the main channel during ordinary floods in single-thread channel configurations. In multi-thread reaches, ordinary floods will tend to deposit LW on bars as well as vegetated and forested islands. Under these circumstances, roughness is the main factor controlling LW deposition. However, the pattern of LW deposition is significantly affected by flood magnitude, and during very extreme floods LW will be retained far away from the main channel, within the active river zone, and on the floodplain in areas covered by meadows and crops characterized by lower roughness values than the areas in the main channel. Therefore, we have demonstrated that LW deposition is not only linked to roughness or to the resistance to flow due to roughness, but it is linked to the relative position of the depositional sites within the river and floodplain, and this is related to the flood magnitude.

In addition, we found a non-uniform spatial distribution of LW deposition (*sensu* Wohl and Beckman, 2014) when comparing both reaches, but also a non-uniform distribution linked to flood magnitude. Therefore, LW deposition is not static but dynamic and will depend on the morphological configuration of the river and the magnitude of a flood event.

Noteworthy, some relevant processes occur at the field scale, such as discharge fluctuations, sediment transport or vegetative regeneration of deposited LW (Gurnell, 2013; Mikuś *et al.*, 2013); these processes are not considered in this study. Our results suggest that in the absence of these processes, LW deposition is controlled by flood magnitude and the flow elevation with respect to the low-flow surface. Further and more detailed investigations including river bed changes, sediment transport, and unsteady flow conditions are therefore needed to enhance these observations.

Little information existed so far on the elevation at which LW is deposited in rivers (Gurnell *et al.*, 2000a; Bertoldi *et al.*, 2013), and this study somewhat closes this gap. Based on results of the model runs, we indicate that the relative elevation of LW deposits differs between floods of different magnitude. We also show that LW is not always deposited in those geomorphic units where the highest roughness values occur as is the case of low-magnitude floods. Instead, we demonstrate that LW deposition will in fact be controlled strongly by water depth. This is due to the fact that the elevation of deposited wood pieces is strongly linked to flood magnitude (Figure 9) and thus to the depth of inundation of particular surfaces in a river reach.

Thanks to the simulation of several flood scenarios and the wood inventories used in this study, we can demonstrate that, along with river reach morphology, flood magnitude has the most significant control on LW deposition. In turn, if only a single flood is analysed, only partial interpretations can be extracted (Bertoldi *et al.*, 2013).

The obtained patterns of LW deposition predicted by the model together with *in situ* observations will increase the understanding of LW dynamics in the Czarny Dunajec River in particular and in other mountain rivers wider than the height of riparian trees (Gurnell *et al.*, 2002; Eaton and Hassan, 2013; Wyżga *et al.*, 2015) in general. In addition, recognition of the factors controlling preferential sites of LW deposition is crucial for the evaluation of flood risks related to LW accumulations in mountain rivers (Kundzewicz *et al.*, 2014). In the future, the use of numerical modelling in combination with field observations could also help to identify the infrastructures most sensitive to the passing of LW, as well as the increase in water level resulting from their blockage and flooded areas nearby.

An improved understanding of LW dynamics seems even more important as LW is nowadays used increasingly in restoration projects aiming to improve the hydromorphological and ecological status of streams and rivers (Kail *et al.*, 2007). At the same time, these projects will be most successful if the re-introduced LW mimics naturally recruited and retained LW. Identifying the preferential sites for LW deposition could therefore aid these restoration works. Especially for the recommended 'passive restoration' methods (i.e. restoring the process of LW recruitment at larger scales rather than placement of LW structures at the reach scale), prediction of preferential depositional sites could be very useful. In addition, the combination of numerical modelling and field data could also help in the design of such projects by testing different scenarios in terms of recruited LW, wood placement at the reach scale and under different magnitude floods.

Conclusions

Understanding LW dynamics – in terms of transport and deposition – is increasingly becoming an issue for practitioners and scientists. The inherent complexity of the processes involved in LW deposition and the lack of long-term observations have usually resulted in a rather fragmentary understanding of the main factors controlling LW retention in rivers. Through the combination of numerical modelling and field observations, we present a wide range of quantitative information on LW deposition. The coupling of approaches illustrated in this paper was performed for most parameters that are likely to influence LW retention in rivers, namely wood size, river morphology, and flood magnitude, and will thus allow quantification of the probability of LW deposition and retention capacity at the reach scale. Through the analysis of two different river reaches with contrasting morphology, we document that preferential sites and depositional probability vary significantly between reaches and flood scenarios. We conclude that the location of LW deposition is mainly controlled by flood magnitude, and therefore deposition is not only influenced by roughness of a given geomorphic unit, as was usually postulated in the past. Instead, we illustrate that flood magnitude exerts control on water depth which, in turn, defines depositional elevation of LW. The findings of this study can likely be considered in a wide range of applications and in regions outside the Polish Carpathians, but clearly also for more studies of similar nature in other rivers for which monitoring data exists.

Acknowledgements—This work was supported by the Polish–Swiss project FLORIST (Flood risk on the northern foothills of the Tatra Mountains; PSPB no. 153/2010). The numerical model used in this study was developed in collaboration with researchers from the Flumen Research Institute (Technical University of Catalunya, Barcelona). The lead author acknowledges Dr Ernest Bladé and Dr Georgina Corestein (Flumen Research Institute) for continuous support. The authors would also like to thank Dr Joanna Zawiejska for her comments and inputs on the early version of the manuscript. The authors thank the editor Professor Stuart Lane, Dr B.C. Eaton and one anonymous reviewer for their helpful comments and suggestions that improved the paper.

References

Abbe TB, Montgomery DR. 2003. Patterns and processes of wood debris accumulation in the Queets river basin, Washington. *Geomorphology* **51**: 81–107.

Beckman ND, Wohl E. 2014. Effects of forest stand age on the characteristics of logjams in mountainous forest streams. *Earth Surface Processes and Landforms* **39**(11): 1421–1431. DOI:10.1002/esp.3531.

Benda L, Hassan MA, Church M, May CL. 2005. Geomorphology of steep land headwaters: The transition from hillslopes to channels. *Journal of the American Water Resources Association* **41**: 835–851.

Bertoldi W, Gurnell AM, Welber M. 2013. Wood recruitment and retention: the fate of eroded trees on a braided river explored using a combination of field and remotely-sensed data sources. *Geomorphology* **180-181**: 146–155.

Bertoldi W, Welber M, Mao L, Zanella S, Comiti F. 2014. A flume experiment on wood storage and remobilization in braided river systems. *Earth Surface Processes and Landforms* **39**: 804–813.

Bladé E, Cea L, Corestein G, Escolano E, Puertas J, Vázquez-Cendón ME, Dolz J, Coll A. 2014. Iber–Herramienta de simulación numérica del flujo en ríos. *Revista Internacional de Metodos Numericos* **30**: 1–10.

Bray DI. 1979. Estimating average velocity in gravel-bed rivers. *Journal of Hydraulics Division, American Society of Civil Engineering* **105**: 1103–1122.

Comiti F, Agostino VD, Moser M, Lenzi MA, Bettella F, Agnese AD, Rigon E, Gius S, Mazzorana B. 2012. Preventing wood-related hazards in mountain basins: from wood load estimation to designing retention structures. In *12th congress INTERPRAEVENT 2012—Grenoble/France conference proceedings*; 651–662.

Comiti F, Andreoli A, Lenzi MA, Mao L. 2006. Spatial density and characteristics of woody debris in five mountain rivers of the Dolomites (Italian Alps). *Geomorphology* **78**: 44–63.

Curran JC. 2010. Mobility of large woody debris (LWD) jams in a low gradient channel. *Geomorphology* **116**: 320–329.

Diez JR, Elosegi A, Pozo J. 2001. Woody debris in north Iberian streams: influence of geomorphology, vegetation, and management. *Environmental Management* **28**: 687–98.

Eaton BC, Hassan MA. 2013. Scale-dependent interactions between wood and channel dynamics: Modeling jam formation and sediment storage in gravel-bed streams. *Journal of Geophysical Research, Earth Surface* **118**: 2500–2508.

Elosegi A, Diez JR, Pozo J. 1999. Abundance, characteristics, and movement of woody debris in four Basque streams. *Archiv für Hydrobiologie* **144**: 455–471.

Gurnell A. 2007. Wood in world rivers. *Earth Surface Processes and Landforms* **32**: 1129–1130.

Gurnell A. 2012. Fluvial geomorphology: wood and river landscapes. *Nature Geoscience* **5**: 93–94.

Gurnell AM. 2003. Wood storage and mobility. In *The Ecology and Management of Wood in World Rivers*, Gregory SV, Boyer KL, Gurnell AM (eds). American Fisheries Society: Bethesda, MD; 75–91.

Gurnell AM. 2013. Wood in fluvial systems. In *Treatise on Geomorphology 9*, Shroder J, Wohl E (eds). Academic Press: San Diego, CA; 163–188.

Gurnell AM, Petts GE, Hannah DM, Smith BPG, Edwards PJ, Kollmann J, Ward JV, Tockner K. 2000a. Wood storage within the active zone of a large European gravel-bed river. *Geomorphology* **34**: 55–72.

Gurnell AM, Petts GE, Harris N, Ward JV, Tockner K, Edwards PJ, Kollmann J. 2000b. Large wood retention in river channels: the case of the Fiume Tagliamento, Italy. *Earth Surface Processes and Landforms* **25**: 255–275.

Gurnell AM, Piégay H, Swanson FJ, Gregory SV. 2002. Large wood and fluvial processes. *Freshwater Biology* **47**: 601–619.

Kail J, Hering D, Muhar S, Gerhard M, Preis S. 2007. The use of large wood in stream restoration: experiences from 50 projects in Germany and Austria. *Journal of Applied Ecology* **44**: 1145–1155.

Kraft CE, Warren DR. 2003. Development of spatial pattern in large woody debris and debris dams in streams. *Geomorphology* **51**: 127–139.

Kundzewicz ZW, Stoffel M, Kaczka RJ, Wyżga B, Niedźwiedź T, Pińskwar I, Ruiz-Villanueva V, Łupikasza E, Czajka B, Ballesteros-Canovas JA, Małarzewski Ł, Choryński A, Janecka K, Mikuś P. 2014. Floods at the northern foothills of the Tatra Mountains – a Polish–Swiss research project. *Acta Geophysica* **62**: 620–641.

Lassettre NS, Dufour S, Rollet A. 2008. Decadal changes in distribution and frequency of wood in a free meandering river, the Ain River, France. *Earth Surface Processes and Landforms* **33**: 1098–1112.

MacVicar BJ, Henderson A, Comiti F, Oberlin C, Pecorari E. 2009. Quantifying the temporal dynamics of wood in large rivers: field trials of wood surveying, dating, tracking, and monitoring techniques. *Earth Surface Processes and Landforms* **34**: 2031–2046.

May CL, Gresswell RE. 2003. Large wood recruitment and redistribution in headwater streams in the southern Oregon Coast Range, USA. *Canadian Journal of Forestry Research* **33**: 1352–1362.

Meyer-Peter E, Müller R. 1948. Formulas for bed-load transport. In *Proceedings of the 2nd Meeting, IAHR*, Stockholm; 39–64.

Mikuś P, Wyżga B, Kaczka RJ, Walusiak E, Zawiejska J. 2013. Islands in a European mountain river: linkages with large wood deposition, flood flows and plant diversity. *Geomorphology* **202**: 115–127.

Montgomery DR, Collins BD, Buffington JM, Abbe TB. 2003. Geomorphic effects of wood in rivers. In *The Ecology and Management of Wood in World Rivers*, Gregory SV, Boyer KL, Gurnell AM (eds). American Fisheries Society: Bethesda, MD; 21–47.

Morris AEL, Goebel PC, Palik BJ. 2009. Spatial distribution of large wood jams in streams related to stream–valley geomorphology and forest age in northern Michigan. *River Research and Applications* **26**: 835–847.

Moulin B, Schenk ER, Hupp CR. 2011. Distribution and characterization of in-channel large wood in relation to geomorphic patterns on a low-gradient river. *Earth Surface Processes and Landforms* **36**: 1137–1151.

Pecorari E. 2008. Il materiale legnoso in corsi d'acqua a canali intrecciati: volumi, mobilita, degradazione ed influenza morfologica, PhD Dissertation. University of Padova.

Piégay H, Thévenet A, Citterio A. 1999. Input, storage and distribution of large woody debris along a mountain river continuum, the Drome River, France. *Catena* **35**: 19–29.

Rigon E, Comiti F, Lenzi M. 2012. Large wood storage in streams of the Eastern Italian Alps and the relevance of hillslope processes. *Water Resources Research* **48** W01518.

Ruiz-Villanueva V, Bladé-Castellet E, Sánchez-Juny M, Martí B, Díez-Herrero A, Bodoque JM. 2014a. Two dimensional numerical modelling of wood transport. *Journal of Hydroinformatics* **16**: 1077–1096.

Ruiz-Villanueva V, Bladé-Castellet E, Díez-Herrero A, Bodoque JM, Sánchez-Juny M. 2014b. Two dimensional modelling of large wood transport during flash floods. *Earth Surface Processes and Landforms* **39**: 438–449.

Ruiz-Villanueva V, Bodoque JM, Díez-Herrero A, Bladé E. 2014c. Large-wood transport as significant influence on flood risk in a mountain village. *Natural Hazards* **74**: 967–987.

Ruiz-Villanueva V, Wyżga B, Zawiejska J, Hajdukiewicz M, Stoffel M. 2015. Factors controlling large-wood transport in a mountain river. *Geomorphology*. DOI:10.1016/j.geomorph.2015.04.004.

Strickler A. 1923. *Beiträge zur Frage der Geschwindigkeitsformel und der Rauhigkeitszahlen fur Ströme, Kanäle und Geschlossene Leitungen*. Amt für Wasserwirtschaft: Bern.

Swanson FJ. 2003. Wood in rivers: a landscape perspective. In *The Ecology and Management of Wood in World Rivers*, Gregory SV, Boyer KL, Gurnell AM (eds). American Fisheries Society: Bethesda, MD; 299–313.

Van der Nat D, Schmidt AP, Tockner K, Edwards PJ, Ward JV. 2002. Inundation dynamics in braided floodplains: Tagliamento River, northeast Italy. *Ecosystems* **5**: 636–647.

Van der Nat D, Tockner K, Edwards PJ, Ward JV, Gurnell AM. 2003. Habitat change in braided flood plains (Tagliamento, NE-Italy). *Freshwater Biology* **48**: 1799–1812.

Welber M, Bertoldi W, Tubino M. 2013. Wood dispersal in braided streams: results from physical modeling. *Water Resources Research* **49**: 7388–7400.

Wohl E. 2013. Floodplains and wood. *Earth-Science Reviews* **123**: 194–212.

Wohl E, Beckman N. 2014. Controls on the longitudinal distribution of channel-spanning logjams in the Colorado Front Range, USA. *River Research and Applications* **131**: 112–131.

Wohl E, Cadol D. 2011. Neighborhood matters: patterns and controls on wood distribution in old-growth forest streams of the Colorado Front Range, USA. *Geomorphology* **125**: 132–146.

Wohl E, Cenderelli DA, Dwire KA, Ryan-Burkett SE, Young MK, Fausch KD. 2010. Large in-stream wood studies: a call for common metrics. *Earth Surface Processes and Landforms* **35**: 618–625.

Wohl E, Jaeger K. 2009. A conceptual model for the longitudinal distribution of wood in mountain streams. *Earth Surface Processes and Landforms* **344**: 329–344.

Wyżga B, Oglęcki P, Radecki-Pawlik A, Skalski T, Zawiejska J. 2012. Hydromorphological complexity as a driver of the diversity of benthic invertebrate communities in the Czarny Dunajec River, Polish Carpathians. *Hydrobiologia* **696**: 29–46.

Wyżga B, Zawiejska J. 2005. Wood storage in a wide mountain river: case study of the Czarny Dunajec, Polish Carpathians. *Earth Surface Processes and Landforms* **30**: 1475–1494.

Wyżga B, Zawiejska J. 2010. Large wood storage in channelized and unmanaged sections of the Czarny Dunajec River, Polish Carpathians: implications for the restoration of mountain rivers. *Folia Geographica, Series Geographica Physica* **41**: 5–34.

Wyżga B, Zawiejska J, Mikuś P, Kaczka RJ. 2015. Contrasting patterns of wood storage in mountain watercourses narrower and wider than the height of riparian trees. *Geomorphology* **228**: 275–285.

Zawiejska J, Wyżga B. 2010. Twentieth-century channel change on the Dunajec River, southern Poland: patterns, causes and controls. *Geomorphology* **117**: 234–246.

Zawiejska J, Wyżga B, Radecki-Pawlik A. 2015. Variation in surface bed material along a mountain river modified by gravel extraction and channelization, the Czarny Dunajec, Polish Carpathians. *Geomorphology* **231**: 353–366.

